Spin-polarized currents driven by spin-dependent surface screening

Piotr Graczyk*
Institute of Molecular Physics, Polish Academy of Sciences, M. Smoluchowskiego 17, 60-179 Poznan, Poland

Maciej Krawczyk†
Faculty of Physics, Adam Mickiewicz University in Poznan, Uniwersytetu Poznańskiego 2, 61-614 Poznan, Poland

(Received 21 February 2019; revised manuscript received 30 October 2019; published 14 November 2019)

We demonstrate the mechanism of spin current generation in ultrathin ferromagnetic film by voltage-induced interface magnetoelectric effect and provide a rigorous theoretical and numerical description of the phenomenon. Surprisingly, for MgO-Cu-Co-MgO systems the spin-dependent screening in thin (less than 20 nm) Co film produces spin accumulation 7 times higher than the accumulation induced by the bulk effect of spin-dependent conductivity in thick Co films. An experimental approach to validate our numerical predictions is proposed. The demonstrated effect opens routes to design highly miniaturized, voltage-controlled spintronic or magnonic devices, while the developed model is a useful tool to study spin currents driven by surface screening.

DOI: 10.1103/PhysRevB.100.195415

I. INTRODUCTION

The phenomenon of spin-dependent surface screening (SS) leads to the charge-mediated magnetoelectric effect (ME), which is the key mechanism for the electric control of magnetic properties in ultrathin multiferroic heterostructures [1,2]. The effect has been described first theoretically by Zhang in 1999 [3] and then confirmed by *ab initio* calculations [4–6]. It has been shown experimentally that SS may be utilized to change the magnetization, anisotropy, or coercivity of ultrathin ferromagnetic film [7–14], to induce magnetic ordering transition [15,16], or even induce surface magnetism in nonmagnetic materials [17]. In multiferroic tunnel junctions SS provides significant contribution to the tunneling resistance [18,19] and opens possibilities to manipulate the spin polarization of tunneling electrons [20,21]. Owing to the surface magnetic anisotropy that is controlled by SS, spin waves may be excited parametrically or resonantly with the ac voltage [22–26].

Spin-dependent surface screening changes the absolute value of magnetization at the dielectric-ferromagnetic metal (D-FM) interface, in contrast to, studied more extensively, strain-driven ME effects [2,27–29], which rotate the magnetization direction. Although strain-driven ME remains significant for relatively thick layers, it suffers from ageing effects, clamping, and integration problems with current technology. Therefore, charge-mediated ME is a more promising mechanism for applications in the nanoscale devices.

In this paper we present that the SS mechanism in an ultrathin ferromagnetic layer leads to generation of the spin-polarized current and spin accumulation in D-FM systems. Therefore it may be regarded as an alternative to the mechanism of current polarization in the conventional spin-transfer torque magnetic random access memory (STT-MRAMs) [30], providing the possibility for further miniaturization of spintronic devices.

We study the spin-dependent surface screening effect in a D-FM-D system subjected to ac voltage. The change of the voltage results in the change of the screening charges at the insulator-ferromagnet interface. Since the screening is spin dependent, we show that this leads to the appearance of nonequilibrium spin density at the interface which generates diffusive spin current. We explain this effect within the Stoner band model and derive the term that describes SS in drift-diffusive formalism. With this model we perform numerical simulations and obtain the spin current with the contributions from spin-dependent conductivity (SC) and SS for a MgO-Cu-Co-MgO system. What is important is that the SS contribution significantly prevails over the SC for systems with an ultrathin Co layer. Finally, we propose the strategy to distinguish experimentally between that two current polarization mechanisms.

The two considered systems are shown in Fig. 1. The multilayers consist of two 2-nm-thick MgO films separated by Co film of different thicknesses. In system A the Co layer is separated from MgO by a 2-nm-thick nonmagnetic metal (Cu) at both interfaces, while in system B it is separated from MgO only from the top. Therefore, in system A there is no D-FM interface, while in system B it is present. Consequently, screening charges will appear in the ferromagnet only at the bottom interface in system B when the voltage is applied to the multilayer structure through bottom and top electrodes (e2 and e1, respectively). It is assumed that charge and spin transport is only perpendicular to the layers along the x axis.

II. DRIFT-DIFFUSION MODEL

The coupled charge-spin dynamics driven by the ac voltage is considered on the base of the diffusive model [31,32]. The

*graczyk@ifmpan.poznan.pl
†krawczyk@amu.edu.pl

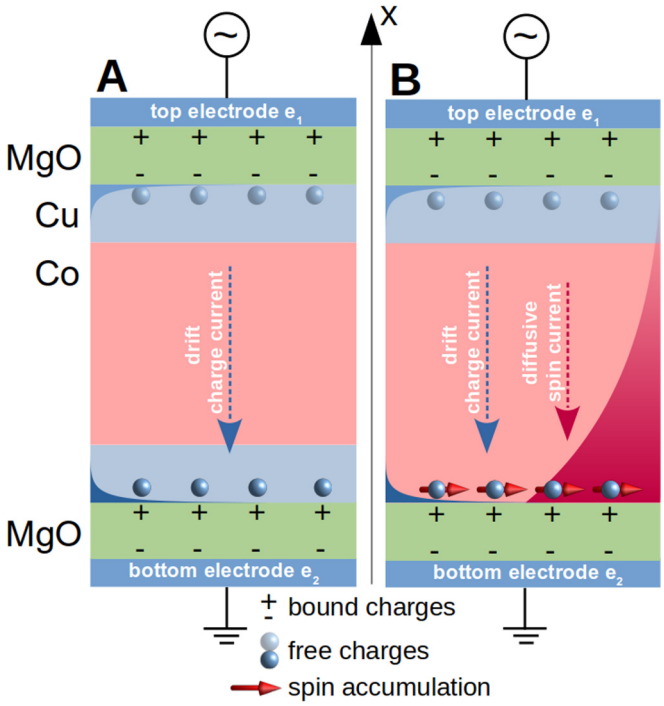

FIG. 1. The schematic of considered composites. In system A there is no D-FM interface, while in system B the single D-FM interface is present. With an ac voltage applied to system B, the spin accumulation appears at the Co/MgO interface as a consequence of the spin-dependent surface screening. The spin accumulation diffuses to the bulk of the metallic multilayer.

free charge density current J_f is described in the metal layers by the equation

$$J_f = \sigma E - D\frac{\partial n_f}{\partial x} + \beta D\frac{e}{\mu_B}\frac{\partial s}{\partial x}, \tag{1}$$

which includes contributions from electron drift driven by the electric field E, diffusion driven by the gradient of free charge density n_f, and diffusive spin polarization representing the SC contribution, respectively. Here, σ is conductivity, D is the diffusion constant, β is the spin asymmetry coefficient, μ_B is Bohr magneton, and e is the electron charge. In dielectric layers the displacement current is described by the equation

$$J_b = \epsilon_0\epsilon_r\frac{\partial E}{\partial t}, \tag{2}$$

where $\epsilon_0\epsilon_r$ is the permittivity of the material. The conservation of free ($i = f$) and bound ($i = b$) charge density n_i is described by the continuity equation:

$$\frac{\partial n_i}{\partial t} = -\frac{\partial J_i}{\partial x}. \tag{3}$$

Electric potential V is given by the Gauss law:

$$\epsilon_0\frac{\partial^2 V}{\partial x^2} = n_f + n_b,$$
$$E = -\frac{\partial V}{\partial x}, \tag{4}$$

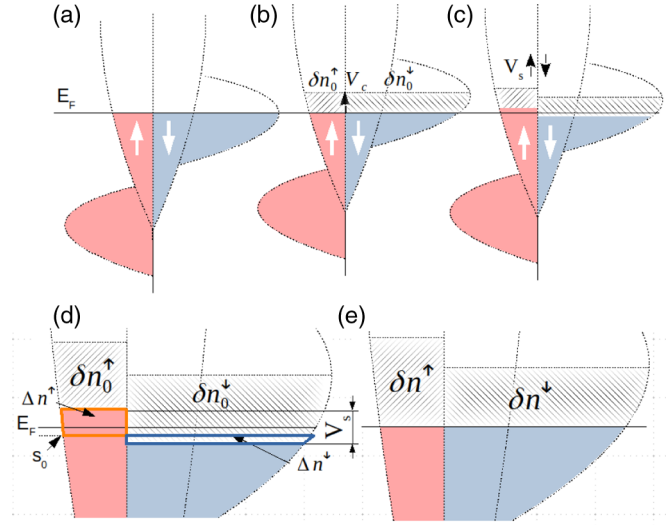

FIG. 2. Schematic diagrams of s and d bands in Co (a) at electric field $E = 0$ and in equilibrium; (b) at $E \neq 0$ with equal band shift $-V_c$; (c) at $E \neq 0$ with screening exchange splitting V_s. (d) Dynamic nonequilibrium charges (with respect to equilibrium spin level s_0) $\Delta n^{\uparrow}$ and $\Delta n^{\downarrow}$ developing as a consequence of the dynamic exchange splitting. In (e) the equilibrium state with the exchange splitting of the screening charges is shown.

with the boundary conditions at the electrodes:

$$V|_{x=e1} = U = U_0\sin(2\pi f_0 t),$$
$$V|_{x=e2} = 0, \tag{5}$$

where f_0 is the frequency of the oscillating voltage U.

The spin current J_s in the ferromagnetic material is modeled by the equation [32]

$$J_s = -D\frac{\partial s}{\partial x} - \beta\frac{\mu_B}{e}\left(\sigma E - D\frac{\partial n_f}{\partial x}\right), \tag{6}$$

which describes spin current driven by the gradient of the spin accumulation s (diffusion) and the spin-conductivity term.

The continuity equation for the spin accumulation s is

$$\frac{\partial s}{\partial t} = -\frac{\partial J_s}{\partial x} - \frac{s}{T_1} + f_s, \tag{7}$$

which describes the rate of change of s due to the gradient of the spin current, the spin-flip relaxation with the characteristic time T_1. f_s is an additional source from spin-dependent surface screening. The formula for f_s is derived below. We use in the following paragraphs $n \equiv n_f$.

III. SPIN-DEPENDENT POTENTIAL AS A SOURCE OF THE NONEQUILIBRIUM SPIN DENSITY

We will consider the voltage-driven magnetization and spin-density change in Co within the Stoner model [33]. Due to the exchange splitting of the band d for the majority and minority spins and partially filled minority subband [Fig. 2(a)] there exists equilibrium spin density (magnetization) in the bulk of the ferromagnet which is equal to the difference between charge densities of the spin-up ($\uparrow$) and spin-down ($\downarrow$) subbands, $m = \mu_B(n^{\uparrow} - n^{\downarrow})/e$. The voltage applied to the

system shifts the potential of the bands at the D-FM interfaces [Fig. 2(b)], leading to the accumulation of the screening charge density $n = \delta n_0^{\uparrow} + \delta n_0^{\downarrow}$ where δn_0^p is accumulated screening charge in the subband p. Since the density of states is different between subbands at the Fermi level ($\Delta\rho = \rho^{\uparrow} - \rho^{\downarrow} < 0$ for Co), then screening charge changes the value of the magnetization at the interface by $\delta m_0 = \mu_B(\delta n_0^{\uparrow} - \delta n_0^{\downarrow})/e$ [4].

Another important feature of the screening in the ferromagnet is that the changes in the band occupancy influence the exchange splitting [5], i.e., the potential is spin dependent [3,18]:

$$V^p = V_c - \frac{I}{e}(\delta n^p - \delta n^{-p}), \tag{8}$$

where I is the exchange constant. Spin-dependent potential (8) means that the subbands shift relative to each other by $V_s = V^{\uparrow} - V^{\downarrow} = -2I\delta m$ [Fig. 2(c)]. From Eqs. (5) and (11) in Ref. [3] we get the relation between V_s and screening charge $n = \delta n^{\uparrow} + \delta n^{\downarrow}$ in the linearized Thomas-Fermi model:

$$V_s = -\frac{2I\Delta\rho}{\rho + 4I\rho^{\uparrow}\rho^{\downarrow}}n, \tag{9}$$

where $\rho = \rho^{\uparrow} + \rho^{\downarrow}$. This shift has important consequences. Since $\rho^{\uparrow} \neq \rho^{\downarrow}$, the shift changes the equilibrium charge level with respect to the Fermi level by $E_F - s_0$ [Fig. 2(d)], where $s_0 = -e(V^{\uparrow}\rho^{\uparrow} + V^{\downarrow}\rho^{\downarrow})/\rho$ is the spin equilibrium level. This leads to the changes in equilibrium charge densities $\delta n^p \neq \delta n_0^p$ and potential V_c. Therefore, the surface magnetization value changes by $\delta m \neq \delta m_0$. Moreover, the screening length in ferromagnet λ_F deviates from the conventional Thomas-Fermi value $\lambda = (\epsilon_0/e^2\rho)^{1/2}$ and thus the capacitance is reduced [3]. We can implement this effect to our numerical model where the screening length is defined as $\lambda = (\epsilon_0 D/\sigma)^{1/2}$ by dividing drift term and multiplying diffusion term in Eq. (2) by $\gamma_n = \lambda_F/\lambda \approx 1.1$ for Co. However, we found that modification of the screening length does not influence the effect of the spin-polarized current generation which is considered here, so it will be neglected from here forward.

Since screening charge and thus V_s [Eq. (9)] is time dependent under the ac voltage, the change of the shift between subbands ΔV_s is the source of nonequilibrium spin density $\Delta s \propto \Delta V_s$. From Fig. 2(d) we see that with respect to s_0,

$$\begin{aligned}\Delta s &= \frac{\mu_B}{e}(\Delta n^{\uparrow} - \Delta n^{\downarrow}) \\ &= \frac{\mu_B}{e}(-eV^{\uparrow} - s_0)\rho^{\uparrow} - \frac{\mu_B}{e}(-eV^{\downarrow} - s_0)\rho^{\downarrow} \\ &= -2\mu_B\Delta V_s\rho^{\uparrow}\rho^{\downarrow}/\rho e.\end{aligned} \tag{10}$$

Taking the time derivatives we get from Eqs. (9) and (10),

$$f_s \equiv \frac{\partial s}{\partial t} = \frac{4I\rho^{\uparrow}\rho^{\downarrow}}{\rho}\frac{\Delta\rho}{\rho + 4I\rho^{\uparrow}\rho^{\downarrow}}\frac{\mu_B}{e}\frac{\partial n}{\partial t} = \gamma_s\frac{\mu_B}{e}\frac{\partial n}{\partial t}. \tag{11}$$

In equilibrium the final change of magnetization $\delta m = \mu_B(\delta n^{\uparrow} - \delta n^{\downarrow})/e$ is a consequence of uniform potential shift of the bands and their relative exchange splitting [Fig. 2(e)].

Equations (2)–(7) with the source term f_s given by Eq. (11) are solved numerically by the finite-element method in COMSOL MULTIPHYSICS with time-varying voltage applied to the electrodes with amplitude $U_0 = 8$ V and frequency $f_0 = 200$ MHz. The equations are implemented with the currents defined as a flux, thus assuring their continuity at interfaces and zero value at outer boundaries. The relative permittivity is $\epsilon_r = 10$ for MgO and $\epsilon_r = 1$ for metals. We assume the conductivity of metals $\sigma = 1.2 \times 10^7$ S/m and the diffusion constant $D = 4 \times 10^{-3}$ m^2/s. The spin asymmetry coefficient for Co is $\beta = 0.5$ [32], and the spin-flip relaxation time is $T_1 = 0.9$ ps [32]. This corresponds to the spin relaxation length of 60 nm, i.e., much larger than the electron mean free path, satisfying the diffusive limit [31,34,35]. The magnetoelectric coefficient calculated from Eq. (11) with $I = 1.25$ eV, $\rho^{\uparrow} = 0.18$ eV^{-1}, $\rho^{\downarrow} = 0.7$ eV^{-1} [3] is $\gamma_s = -0.25$. We assume also the magnetization of Co film lies in the plane of the film.

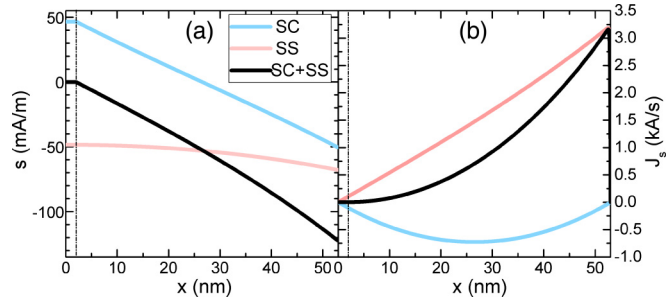

FIG. 3. Spatial distribution of (a) spin accumulation s and (b) spin current J_s through the thickness of the Cu-Co bilayer in the system B with separated contributions from spin-dependent conductivity (SC) and spin-dependent surface screening (SS). The vertical dash-dotted line indicates the Cu/Co interface.

IV. RESULTS

A. The peculiarities of spin transport driven by spin-dependent screening and spin-dependent conductivity

Figure 3 shows the calculated spatial distribution of spin accumulation s and spin current J_s (for system B and thickness of Co film $L_F = 51$ nm) at the moment when they reach maximum values, i.e., when V crosses zero value and charge current flows in the $+x$ direction. We separated the contributions which originate from SC and SS. Since $\beta > 0$, then $\tau_- > \tau_+$, i.e., the relaxation time for spin down is longer than for spin up, and for the current driven by the spin-dependent conductivity there is more spin-down electrons flowing than spin-up electrons. Consequently, J_s has negative sign [Fig. 3(b), blue line] and its maximum is at the center of Cu/Co bilayer. Within the distance proportional to the spin-diffusion length ($L_{sf} = 60$ nm for Co), from the ferromagnet surfaces there builds up a negative spin accumulation gradient [Fig. 3(a), blue line] that stands against the SC term [compare Eq. (6)] [36]. In the Cu layer there is a weak exponential decay of s from the Cu-Co interface.

For the current driven by the spin-dependent surface screening, the outflow of negative charges from the F-D interface generates negative spin accumulation since $\gamma_s < 0$ [Fig. 3(a), red line]. The resulting spin accumulation gradient induces spin current in the direction $+x$ [Fig. 3(b), red line]. The maximum value of J_s is at the D-FM interface.

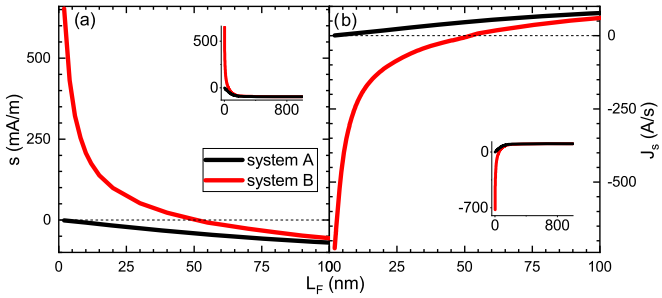

FIG. 4. (a) Spin accumulation and (b) spin current in the Cu layer in dependence on the thickness of the Co layer for system A and system B. The insets show the same dependences but with the extended scale.

The results presented above demonstrate that the spin current driven by SS is a consequence of the spin accumulation gradient buildup. This is in contrast to the SC-polarized current, where the spin accumulation gradient is a result of this current and stands against it.

The effects from SS and SC sum up to give a resultant spin accumulation and spin current (black lines in Fig. 3). In Co ($\beta > 0$, $\gamma_s < 0$) they add up destructively, and for a Co thickness of 51 nm discussed above, that contribution balances out at the Cu layer as shown at the left-hand side of the dash-dotted line in Fig. 3(b).

B. Separation of spin accumulation sources

To clearly distinguish between SC- and SS-generated spin currents we can compare samples where SS would be absent (system A) and samples where SS are present (system B). Moreover, spin-dependent conductivity is a phenomenon that acts in the bulk of the FM material, while the spin-dependent surface screening is an interface effect. Thus, in a thick ferromagnetic layer SC shall dominate while SS should manifest itself in thin ferromagnetic layers.

To prove this, we consider the values of spin accumulation and spin current in the top Cu layer, in dependence on the thickness of Co layer. The black lines in Fig. 4 show s and J_s calculated for the system A. Since there is no D-FM interface, the spin polarization of the current is a result of spin-dependent conductivity only. For a thin Co layer ($L_F < 2L_{sf}$) the spin accumulation counteracts the spin current significantly. For thickness larger than $2L_{sf}$, the influence of the interfacial accumulation loses its significance, and the values of s and J_s saturate with increasing thickness of Co films (see insets in Fig. 4), reaching maximum value of 105 A/s in Cu (and the value of $J_s \approx -\beta J_f = 7000$ A/s in the bulk of Co layer).

The red lines in Fig. 4 show s and J_s for system B. Because of the D-FM interface, there are contributions both from SC and SS to the spin transport. Spin-dependent conductivity dominates for $L_F > L_{sf}$. If the distance from the D-FM interface to the Cu layer is less than $2L_{sf}$, the currents induced by spin-dependent surface screening start to play a significant role and the values of s and J_s deviate from those for system A. At $L_F = 51$ nm SS balances out the SC contribution in Cu, and for $L_F < 51$ nm the spin current driven by SS dominates. The maximum values obtained for $L_F = 2$ nm are $s = 650$ mA/m and $J_s = 730$ A/s, which are 7 times higher than those obtained for thick Co films with dominating spin-dependent conductivity.

The presented dependences of s and J_s on L_F give us a simple tool to distinguish between SS- and SC-driven currents experimentally. If the SS contribution is absent in the system, then $s \to 0$ and $J_s \to 0$ as $L_F \to 0$ (when $L_F < L_{sf}$). If the SS contribution is nonzero, s and J_s tend to nonzero values as $L_F \to 0$ for $L_F < L_{sf}$. It is rather crucial to choose a ferromagnet with a relatively long spin-diffusion length like Co, since the effect is hard to resolve for $L_F > L_{sf}$.

The proposed systems and the method of extraction of SS-driven spin accumulation is suitable to be verified by x-ray magnetic circular dichroism (XMCD) [37,38], where the measurement of spin accumulation dynamics is element-specific and thus may be constrained to the signal from Cu layer. The time-resolved XMCD experiment can distinguish the spin accumulation in the Cu layer generated by the spin-dependent surface screening from that generated by the spin-dependent conductivity, taking into account the dependence of the value of spin accumulation on the Co layer thickness. One then needs the series of samples of different Co layer thicknesses. The spin accumulation will tend to zero in a Cu layer with decreasing Co layer thickness if the spin-dependent surface screening is absent like in system A [black line in Fig. 4(a)]. The spin accumulation will tend to a nonzero value in the Cu layer if the spin-dependent surface screening is present like in system B [red line in Fig. 4(a)].

V. SUMMARY

In summary, the mechanism of spin current generation by the spin-dependent surface screening effect has been proposed and described within the Stoner model. The mechanism has been implemented to the drift-diffusion model. Then the specific dielectric-ferromagnetic heterostructures have been considered numerically to show the properties of SS-driven spin currents. We found the spin accumulation and the spin polarization of the current driven by spin-dependent surface screening is 7 times higher for a 2-nm-thick Co layer than those obtained by spin-dependent conductivity for relatively thick Co layers, e.g., like those used in STT-MRAMs. Since the strength of the effect depends on the density of the screening charge at the dielectric-ferromagnet interface, it can be enhanced with the use of dielectrics or magnetodielectrics of high permittivity [39]. Furthermore, it can be linearly tuned by the change of frequency or amplitude of the ac voltage. The mechanism of SS-driven spin currents can find broad applications in spintronics and magnonics, in particular, through amplifying spin waves through spin currents induced after application of the ac voltage to the multilayered structure.

ACKNOWLEDGMENT

This study has received financial support from the National Science Centre of Poland under Grant No. 2018/28/C/ST3/00052.

[1] J. D. Burton and E. Y. Tsymbal, Magnetoelectric interfaces and spin transport, Philos. Trans. R. Soc., A **370**, 4840 (2012).

[2] C. A. F. Vaz, Electric field control of magnetism in multiferroic heterostructures, J. Phys.: Condens. Matter **24**, 333201 (2012).

[3] S. Zhang, Spin-Dependent Surface Screening in Ferromagnets and Magnetic Tunnel Junctions, Phys. Rev. Lett. **83**, 640 (1999).

[4] C.-G. Duan, J. P. Velev, R. F. Sabirianov, Z. Zhu, J. Chu, S. S. Jaswal, and E. Y. Tsymbal, Surface Magnetoelectric Effect in Ferromagnetic Metal Films, Phys. Rev. Lett. **101**, 137201 (2008).

[5] M. K. Niranjan, J. D. Burton, J. P. Velev, S. S. Jaswal, and E. Y. Tsymbal, Magnetoelectric effect at the $SrRuO_3/BaTiO_3$ (001) interface: An *ab initio* study, Appl. Phys. Lett. **95**, 052501 (2009).

[6] J. M. Rondinelli, M. Stengel, and N. A. Spaldin, Carrier-mediated magnetoelectricity in complex oxide heterostructures, Nat. Nanotechnol. **3**, 46 (2008).

[7] H. J. A. Molegraaf, J. Hoffman, C. A. F. Vaz, S. Gariglio, D. Van Der Morel, C. H. Ahn, and J. M. Triscone, Magnetoelectric effects in complex oxides with competing ground states, Adv. Mater. **21**, 3470 (2009).

[8] M. Weisheit, S. Fähler, A. Marty, Y. Souche, C. Poinsignon, and D. Givord, Electric field-induced modification of magnetism in thin-film ferromagnets, Science **315**, 349 (2007).

[9] T. Maruyama, Y. Shiota, T. Nozaki, K. Ohta, N. Toda, M. Mizuguchi, A. A. Tulapurkar, T. Shinjo, M. Shiraishi, S. Mizukami, Y. Ando, and Y. Suzuki, Large voltage-induced magnetic anisotropy change in a few atomic layers of iron, Nat. Nanotechnol. **4**, 158 (2009).

[10] M. Endo, S. Kanai, S. Ikeda, F. Matsukura, and H. Ohno, Electric-field effects on thickness dependent magnetic anisotropy of sputtered $MgO/Co_{40}Fe_{40}B_{20}/Ta$ structures, Appl. Phys. Lett. **96**, 212503 (2010).

[11] Y. Shiota, T. Maruyama, T. Nozaki, T. Shinjo, M. Shiraishi, and Y. Suzuki, Voltage-assisted magnetization switching in ultrathin $Fe_{80}Co_{20}$ alloy layers, Appl. Phys. Express **2**, 063001 (2009).

[12] Y. Shiota, T. Nozaki, F. Bonell, S. Murakami, T. Shinjo, and Y. Suzuki, Induction of coherent magnetization switching in a few atomic layers of FeCo using voltage pulses, Nat. Mater. **11**, 39 (2011).

[13] T. Seki, M. Kohda, J. Nitta, and K. Takanashi, Coercivity change in an FePt thin layer in a Hall device by voltage application, Appl. Phys. Lett. **98**, 212505 (2011).

[14] D. Chiba, S. Fukami, K. Shimamura, N. Ishiwata, K. Kobayashi, and T. Ono, Electrical control of the ferromagnetic phase transition in cobalt at room temperature, Nat. Mater. **10**, 853 (2011).

[15] J. D. Burton and E. Y. Tsymbal, Prediction of electrically induced magnetic reconstruction at the manganite/ferroelectric interface, Phys. Rev. B **80**, 174406 (2009).

[16] C. A. F. Vaz, J. Hoffman, Y. Segal, J. W. Reiner, R. D. Grober, Z. Zhang, C. H. Ahn, and F. J. Walker, Origin of the Magnetoelectric Coupling Effect in PZT/LSMO Multiferroic Heterostructures, Phys. Rev. Lett. **104**, 127202 (2010).

[17] Y. Sun, J. D. Burton, and E. Y. Tsymbal, Electrically driven magnetism on a Pd thin film, Phys. Rev. B **81**, 064413 (2010).

[18] M. Ye. Zhuravlev, S. Maekawa, and E. Y. Tsymbal, Effect of spin-dependent screening on tunneling electroresistance and tunneling magnetoresistance in multiferroic tunnel junctions, Phys. Rev. B **81**, 104419 (2010).

[19] Y. W. Yin, M. Raju, W. J. Hu, J. D. Burton, Y.-M. Kim, A. Y. Borisevich, S. J. Pennycook, S. M. Yang, T. W. Noh, A. Gruverman, X. G. Li, Z. D. Zhang, E. Y. Tsymbal, and Q. Li, Multiferroic tunnel junctions and ferroelectric control of magnetic state at interface (invited), J. Appl. Phys. **117**, 172601 (2015).

[20] D. Pantel, S. Goetze, D. Hesse, and M. Alexe, Reversible electrical switching of spin polarization in multiferroic tunnel junctions, Nat. Mater. **11**, 289 (2012).

[21] C. Sen, W. A. S. Aldulaimi, O. Mohammadmoradi, and I. B. Misirlioglu, Loss of spin polarization in ferromagnet/ferroelectric tunnel junctions due to screening effects, J. Phys. D: Appl. Phys. **52**, 015305 (2019).

[22] B. Rana, Y. Fukuma, K. Miura, H. Takahashi, and Y. Otani, Excitation of coherent propagating spin waves in ultrathin CoFeB film by voltage-controlled magnetic anisotropy, Appl. Phys. Lett. **111**, 052404 (2017).

[23] R. Verba, V. Tiberkevich, I. Krivorotov, and A. Slavin, Parametric Excitation of Spin Waves by Voltage-Controlled Magnetic Anisotropy, Phys. Rev. Appl. **1**, 044006 (2014).

[24] R. Verba, M. Carpentieri, G. Finocchio, V. Tiberkevich, and A. Slavin, Excitation of Spin Waves in an In-Plane-Magnetized Ferromagnetic Nanowire Using Voltage-Controlled Magnetic Anisotropy, Phys. Rev. Appl. **7**, 064023 (2017).

[25] Y.-J. Chen, H. K. Lee, R. Verba, J. A. Katine, I. Barsukov, V. Tiberkevich, J. Q. Xiao, A. N. Slavin, and I. N. Krivorotov, Parametric resonance of magnetization excited by electric field, Nano Lett. **17**, 572 (2017).

[26] T. Nozaki, Y. Shiota, S. Miwa, S. Murakami, F. Bonell, S. Ishibashi, H. Kubota, K. Yakushiji, T. Saruya, A. Fukushima, S. Yuasa, T. Shinjo, and Y. Suzuki, Electric-field-induced ferromagnetic resonance excitation in an ultrathin ferromagnetic metal layer, Nat. Phys. **8**, 491 (2012).

[27] P. Graczyk, R. Schäfer, and B. Mroz, Magnetoelastic coupling between NiFe thin film and LiCsSO4 studied by Kerr microscopy, J. Phys. D: Appl. Phys. **48**, 425002 (2015).

[28] P. Graczyk, A. Trzaskowska, K. Zaleski, and B. Mroz, Tunable properties of spin waves in magnetoelastic NiFe/GMO heterostructure, Smart Mater. Struct. **25**, 075017 x (2016).

[29] P. Graczyk, A. Trzaskowska, K. Adrjanowicz, B. Peplinska, and B. Mroz, Large magnetoelastic coupling in $NiFe/LiCsSO_4$ and $NiFe/KH_2PO_4$ heterostructures, J. Alloys Compd. **656**, 825 (2016).

[30] D. Apalkov, A. Ong, A. Driskill-Smith, M. Krounbi, A. Khvalkovskiy, S. Watts, V. Nikitin, X. Tang, D. Lottis, K. Moon, X. Luo, and E. Chen, Spin-transfer torque magnetic random access memory (STT-MRAM), ACM J. Emerg. Technol. Comput. Syst. **9**, 1 (2013).

[31] T. Valet and A. Fert, Theory of the perpendicular magnetoresistance in magnetic multilayers, Phys. Rev. B **48**, 7099 (1993).

[32] Y.-H. Zhu, B. Hillebrands, and H. C. Schneider, Signal propagation in time-dependent spin transport, Phys. Rev. B **78**, 054429 (2008).

[33] E. C. Stoner, Collective electron ferromagnetism, Philos. Trans. R. Soc. A **165**, 372 (1938).

[34] D. R. Penn and M. D. Stiles, Spin transport for spin diffusion lengths comparable to mean free paths, Phys. Rev. B **72**, 212410 (2005).

[35] M. Gmitra and J. Barnaś, Correlation of the angular dependence of spin-transfer torque and giant magnetoresistance in the limit of diffusive transport in spin valves, Phys. Rev. B **79**, 012403 (2009).

[36] V. Zayets, Spin and charge transport in materials with spin-dependent conductivity, Phys. Rev. B **86**, 174415 (2012).

[37] R. Kukreja, S. Bonetti, Z. Chen, D. Backes, Y. Acremann, J. A. Katine, A. D. Kent, H. A. Dürr, H. Ohldag, and J. Stöhr, X-ray Detection of Transient Magnetic Moments Induced by a Spin Current in Cu, Phys. Rev. Lett. **115**, 096601 (2015).

[38] J. Li, L. R. Shelford, P. Shafer, A. Tan, J. X. Deng, P. S. Keatley, C. Hwang, E. Arenholz, G. van der Laan, R. J. Hicken, and Z. Q. Qiu, Direct Detection of Pure ac Spin Current by X-Ray Pump-Probe Measurements, Phys. Rev. Lett. **117**, 076602 (2016).

[39] E. Coy, I. Fina, K. Załęski, A. Krysztofik, L. Yate, L. Rodriguez, P. Graczyk, H. Głowiński, C. Ferrater, J. Dubowik, and M. Varela, High-temperature Magnetodielectric $Bi(Fe_{0.5}Mn_{0.5})O_3$ Thin Films with Checkerboard-Ordered Oxygen Vacancies and Low Magnetic Damping, Phys. Rev. Appl. **10**, 054072 (2018).